Received February 19, 2018, accepted March 12, 2018, date of publication April 6, 2018, date of current version April 25, 2018.

*Digital Object Identifier 10.1109/ACCESS.2018.2820746*

# Statistical Properties of Double Hoyt Fading With Applications to the Performance Analysis of Wireless Communication Systems

**NAZIH HAJRI[1], NEJI YOUSSEF[1], TSUTOMU KAWABATA[2], (Member, IEEE), MATTHIAS PÄTZOLD[3], (Senior Member, IEEE), AND WIEM DAHECH[1]**

[1]Université de Carthage, Ecole Supérieure des Communications de Tunis, Tunis 2083, Tunisia
[2]Department of Communication Engineering and Informatics, University of Electro-Communications, Tokyo 182-8585, Japan
[3]Faculty of Engineering and Science, University of Agder, NO-4898 Grimstad, Norway

Corresponding author: Nazih Hajri (nazih.hajri@supcom.rnu.tn)

**ABSTRACT** In this paper, we investigate the statistical properties of double Hoyt fading channels, where the overall received signal is determined by the product of two statistically independent but not necessarily identically distributed single Hoyt processes. Finite-range integral expressions are first derived for the probability density function (PDF), cumulative distribution function (CDF), level-crossing rate (LCR), and average duration of fades of the envelope fading process. A closed-form approximate solution is also deduced for the LCR by making use of the Laplace approximation theorem. Applying the derived PDF of the double Hoyt channel, we then provide analytical expressions for the average symbol error probability of both coherent M-ary phase-shift keying and square M-ary quadrature amplitude modulation schemes. It is shown that all the obtained theoretical results include those that are already known for double Rayleigh channels as a special case. In addition, simplified expressions for the Hoyt×Rayleigh, Rayleigh×one-sided Gaussian, and double one-sided Gaussian channels are presented. Moreover, the applicableness of the proposed model to measured real-world propagation channels is examined and discussed by comparing the derived CDF and LCR with published measurement data collected in inter-vehicular propagation environments. Numerical and simulation results are also provided to confirm the validity of the derivations.

**INDEX TERMS** Double Hoyt fading channel model, vehicular-to-vehicular (V2V) channels, probability density function (PDF), cumulative distribution function (CDF), level-crossing rate (LCR), average duration of fades (ADF), symbol error probability (SEP).

## I. INTRODUCTION

Double-scattering fading channels can statistically be modeled by a product of two classical fading processes. Research in this area has attracted much interest in recent years. Measurement campaigns and theoretical studies have demonstrated that these kinds of stochastic channels are useful for the modeling of specific multipath propagation channels, such as keyhole channels [2], [3] and street corner channels [4]. The underlying modeling concept is also suitable for the development of mobile-to-mobile (M2M) channels [5]–[7], vehicular-to-vehicular (V2V) channels [8]–[10], dual-hop cooperative relaying channels [11]–[14], and radio frequency identification channels [15], [16]. Numerous works are available in the recent literature which are devoted to the statistical characterization of cascaded fading channels and the related performance analysis. For instance, the first- and second-order statistics of double Rayleigh fading channels have been investigated in [7] and [13]. Cascaded Weibull fading channels have been introduced and analyzed in [17]. In [18], analytical expressions have been derived for the main statistical properties of double Rice fading channels, such as the mean value, variance, probability density function (PDF), level-crossing rate (LCR), and average duration of fades (ADF). Theoretical results for the general case of $N$ multihop Rayleigh ($N*$Rayleigh) channels and $N$ multihop Nakagami-$m$ ($N*$Nakagami-$m$) channels have been reported in [4], [19], and [20], respectively, where $N$ is the number of independent and not necessarily identically Rayleigh (or Nakagami-$m$) random processes. Recently, simple and approximate closed-form expressions for the LCR and ADF

of double Nakagami-$m$ processes have been presented in [21]. Additionally, Peppas *et al.* [22] introduced the so-called cascaded generalized-K fading model, which is constructed as the product of $N$ independent but not necessarily identically distributed squared generalized-K random variables, and analyzed their main statistical properties. Furthermore, Chau and Huang [23] studied the second-order statistics of two correlated double Rayleigh fading channels. More recently, in [24], the product of $N$ Nakagami-$m$ random processes has been approximated by a log-normal process, and approximate closed-form expressions have been determined for the corresponding LCR and ADF.

From the literature above, it can be noted that all the published works on the statistical properties of cascaded fading channels have only considered models grounded on widely accepted distributions, namely the Rayleigh, Weibull, Rice, Nakagami-$m$, and generalized-K distributions. Besides all these classical distributions, the Hoyt (also referred to as Nakagami-$q$) model [25]–[27], where $q$ ($0 \leq q \leq 1$) is called the Hoyt fading severity parameter, has attracted the attention of many researchers in recent years. This model offers a high degree of flexibility in that it allows to describe fading conditions which are more severe than those described by the Rayleigh fading model. In fact, the Hoyt channel includes the Rayleigh channel ($q = 1$) and the one-sided Gaussian channel ($q = 0$) as special cases [27], [28]. Furthermore, the complex channel gain can be expressed in terms of Gaussian processes, making the Hoyt model attractive in simulation based performance studies. The statistical characterization of Hoyt fading channels and performance analysis of digital communication schemes over such channels have widely been studied in the literature. For example, the main statistical properties of single Hoyt fading channels have been reported in [25], [27], [29], and [30]. Important studies dealing with the performance analysis of wireless transmission schemes over such channel have been reported in [30]–[33]. An expression for the bivariate Hoyt distribution assuming arbitrarily correlation pattern in non-stationary environments has recently been derived in [34].

Motivated by the appropriateness of double fading channel models for the modeling of double scattering scenarios in V2V communications, and strengthened by the attractive features of the Hoyt fading model, we investigate in this paper the statistics of double Hoyt fading channels and analyze the symbol error probability (SEP) performance of coherent M-ary phase-shift keying (M-PSK) and square M-ary quadrature amplitude modulation (M-QAM) schemes. The underlying channel model is sufficiently generic as it includes the double Rayleigh, double one-sided Gaussian, Hoyt×Rayleigh (or Rayleigh×Hoyt), Hoyt×one-sided Gaussian (or one-sided Gaussian×Hoyt), Rayleigh×one-sided Gaussian (or one-sided Gaussian×Rayleigh) fading channels as special cases. This implies that the results presented in this work encompass all results obtained for these special cases.

Specifically, we provide theoretical expressions for the PDF, CDF, LCR, and ADF of double Hoyt fading processes, which are defined by the product of two independent but not necessarily identically distributed single Hoyt fading processes. Apart from the channel statistics, the focus of this paper is also on the error performance analysis of wireless communications over double Hoyt fading channels. By making use of the derived expression for the PDF of the underlying double Hoyt fading process, the investigation of analytical expressions for the SEP is carried out for both coherent M-PSK and square M-QAM modulation schemes under the assumption of quasi-static channel conditions, i.e., the instantaneous signal-to-noise ratio (SNR) remains constant over the symbol duration and changes randomly from one symbol to the next one. The derived expressions for the first-order statistics of the envelope fading process as well as the SEP are given in terms of finite-range integrals of trigonometric functions that are easy to calculate numerically. Concerning the analytical solutions for the LCR and ADF, they involve finite- and semi-infinite range integrals. To make the LCR and ADF computationally tractable, closed-form approximate solutions have been derived for these statistical quantities by applying the Laplace approximation theorem [35]. It is shown that all the derived analytical quantities include the corresponding results that are already known for double Rayleigh fading channels. Additionally, simple analytical expressions are deduced for asymmetrical double fading channels described by the compound Hoyt×Rayleigh (or Rayleigh×Hoyt) channels. The obtained results are also valid for double one-sided Gaussian, Hoyt×one-sided Gaussian, and Rayleigh×one-sided Gaussian channels, which are considered as limiting cases of the double Hoyt model. Moreover, the applicability of the model to the characterization of real-word channels is examined by comparing the CDF and LCR of the double Hoyt fading envelope with that of measurement data collected in inter-vehicular channels reported in [8]. Finally, the validity of the derived analytical results is verified by means of simulations. Drawing upon the results on the envelope of double Hoyt fading channels, derived in this paper, analytical expressions for the PDF, CDF, LCR, and ADF of the associated instantaneous channel capacity can also be investigated.

The remainder of the paper is organized as follows. Section II presents a description of the double Hoyt fading channel model followed by the derivation of the characteristic function (CF) and the PDF of the quadrature components of the complex channel gain as well as the PDF and CDF of the double Hoyt process. Exact and closed-form approximate expressions are investigated in Section III for the LCR and ADF of double Hoyt processes. The SEP performance analysis of M-PSK and square M-QAM modulation schemes is provided in Section IV. Section V contains numerical and simulation results along with the fitting of the CDF and LCR to measurement data on inter-vehicular channels. Finally, the conclusion is outlined in Section VI.

## II. FIRST-ORDER STATISTICS OF DOUBLE HOYT MULTIPATH FADING CHANNELS

In double Hoyt fading environments, the complex channel gain is described under narrow-band conditions by the product of two statistically independent but not necessarily identically distributed zero-mean complex Gaussian processes according to

$$\begin{aligned} Z(t) &= (X_1(t) + jY_1(t))(X_2(t) + jY_2(t)) \\ &= X_1(t)X_2(t) - Y_1(t)Y_2(t) \\ &\quad + j(X_1(t)Y_2(t) + X_2(t)Y_1(t)) \\ &= Z_1(t) + jZ_2(t) \end{aligned} \tag{1}$$

where $X_i(t)$ and $Y_i(t)$ are real valued zero-mean Gaussian processes with variances $\sigma_{X_i}^2$ and $\sigma_{Y_i}^2$ $(i = 1, 2)$, respectively, which are not necessarily identical. The overall fading envelope $R(t)$ of the underlying double Hoyt channel is defined as

$$R(t) = R_1(t)R_2(t). \tag{2}$$

In (2), $R_i(t) = \sqrt{X_i^2(t) + Y_i^2(t)}$ $(i = 1, 2)$ is a Hoyt process, the PDF of which is given by [25]

$$\begin{aligned} p_{R_i}(z) = \left(\frac{1+q_i^2}{q_i\Omega_i}\right) z \exp\left[-\frac{z^2}{4\Omega_i}\left(\frac{1+q_i^2}{q_i}\right)^2\right] \\ \times I_0\left[\frac{z^2}{4\Omega_i}\left(\frac{1-q_i^4}{q_i^2}\right)\right], \quad z \geq 0 \end{aligned} \tag{3}$$

where $\Omega_i = \mathrm{E}(R_i^2) = \sigma_{X_i}^2 + \sigma_{Y_i}^2$, in which $\mathrm{E}(\cdot)$ represents the expectation operator, and $I_0(\cdot)$ is the modified Bessel function of the first-kind. Also in (3), $q_i \in [0, 1]$ denotes the Hoyt fading parameter that is defined in terms of the variances $\sigma_{X_i}^2$ and $\sigma_{Y_i}^2$ as $q_i = \sigma_{X_i}/\sigma_{Y_i}$ if $\sigma_{Y_i} \geq \sigma_{X_i}$, and as $q_i = \sigma_{Y_i}/\sigma_{X_i}$ in the case where $\sigma_{X_i} \geq \sigma_{Y_i}$. Here, we assume that $\sigma_{X_i} \geq \sigma_{Y_i}$ $(i = 1, 2)$.

In this section, our major focus is on the determination of the PDF and CDF of the double Hoyt process $R(t)$, which are important for the performance analysis of wireless communications. Prior to that, however, we investigate the first-order statistics of the in-phase and quadrature components of the complex faded envelope $Z(t)$. The statistics of these quadrature components are of relevance for, e.g., the determination of the statistics of the channel envelope and phase, and the derivation and performance assessment of channel simulators [30]. The analysis will be carried out under the assumption of independent complex channel gains $X_i(t) + jY_i(t)$ $(i = 1, 2)$, which are not necessarily identically distributed.

### A. STATISTICS OF $Z_i(t)$

As can be noted from (1), the stochastic process $Z_i(t)$ $(i = 1, 2)$ is written as the sum of the product of two independent Gaussian processes. From [36, eq. (6.2)], the PDF of the process $X(t) = X_1(t)X_2(t)$ is given by $p_X(x) = K_0(|x|/(\sigma_{X_1}\sigma_{X_2}))/(\pi\sigma_{X_1}\sigma_{X_2})$, where $K_0(\cdot)$ is the zeroth-order modified Bessel function of the second kind [38]. The CF of the process $X(t)$ is given by $\psi_X(\omega) = 1/\sqrt{1 + \sigma_{X_1}^2\sigma_{X_2}^2\omega^2}$ [36, eq. (6.4)]. The PDFs and CFs of the other product Gaussian processes appearing in (1) are expressed in a similar manner as above, except that the standard deviations $\sigma_{X_1}$ and $\sigma_{X_2}$ have to be replaced by the associated quantities. Thus, as the two products of the Gaussian processes of the real part of (1) are statistically independent, it follows that the CF of $Z_1(t) = X_1(t)X_2(t) - Y_1(t)Y_2(t)$ can be written as

$$\psi_{Z_1}(\omega) = \frac{1}{(1 + \sigma_{X_1}^2\sigma_{X_2}^2\omega^2)^{1/2}(1 + \sigma_{Y_1}^2\sigma_{Y_2}^2\omega^2)^{1/2}}. \tag{4}$$

Analogously, the CF of $Z_2(t) = X_1(t)Y_2(t) + X_2(t)Y_1(t)$ is given by

$$\psi_{Z_2}(\omega) = \frac{1}{(1 + \sigma_{X_1}^2\sigma_{Y_2}^2\omega^2)^{1/2}(1 + \sigma_{X_2}^2\sigma_{Y_1}^2\omega^2)^{1/2}}. \tag{5}$$

Now, the PDF of $Z_i(t)$ $(i = 1, 2)$ can be obtained via the inverse Fourier transform of the CF $\psi_{Z_i}(\omega)$ according to [36]

$$\begin{aligned} p_{Z_i}(z) &= \frac{1}{2\pi}\int_{-\infty}^{\infty} \psi_{Z_i}(\omega)\exp(-j\omega z)d\omega \\ &= \frac{1}{\pi}\int_0^{\infty} \psi_{Z_i}(\omega)\cos(\omega z)d\omega. \end{aligned} \tag{6}$$

Unfortunately, there is no closed-form solution for the integral in (6). However, a closed-form solution to the PDF $p_{Z_2}(z)$ of $Z_2(t)$ can be obtained for the special case of $\sigma_{X_1}\sigma_{Y_2} = \sigma_{X_2}\sigma_{Y_1} = \sigma_Q$, i.e., $q_1 = q_2$. In this case, the integral in (6), after the insertion of (5), can be solved with the help of [38, eq. (3.723.2)], leading to

$$p_{Z_2}(z) = \frac{1}{2\sigma_Q}\exp\left(-\frac{|z|}{\sigma_Q}\right). \tag{7}$$

The result above states that $Z_2(t)$ follows the Laplace distribution with the parameter $\sigma_Q$, i.e., $Z_2(t) \sim L(0, \sigma_Q)$. Note that this statistics holds true for $Z_1(t)$ only if $\sigma_{X_1}\sigma_{X_2} = \sigma_{Y_1}\sigma_{Y_2}$, i.e., $q_1 = 1/q_2$. In this situation, however, the constraint $q_i \leq 1$ cannot be fulfilled simultaneously for both $q_1$ and $q_2$, which means that the underlying statistical property cannot be valid for $Z_1(t)$. Finally, for $\sigma_{X_i} = \sigma_{Y_i} = \sigma$, i.e., $q_i = 1$ $(i = 1, 2)$, the statistics of $Z_1(t)$ and $Z_2(t)$ are described by the Laplace distribution $L(0, \sigma)$ which is the known result for double Rayleigh fading channels [13, eq. (5)].

In the sequel, we investigate the PDF and CDF of the envelope process $R(t)$, which are of relevance for the performance analysis.

### B. PDF AND CDF OF THE DOUBLE HOYT PROCESS $R(t)$

Owing to the fact that the Gaussian processes $X_i(t)$ and $Y_i(t)$ are assumed to be statistically independent, it follows that the processes $R_1(t)$ and $R_2(t)$ are also statistically independent. As a starting point for the derivation of the PDF of the double Hoyt process $R(t) = R_1(t)R_2(t)$, we may use the fact that the PDF of the product of the two independent processes $R_1(t)$

and $R_2(t)$ can be expressed as follows [37]

$$p_R(z) = \int_{-\infty}^{\infty} \frac{1}{|y|} p_{R_1 R_2}\left(\frac{z}{y}, y\right) dy \tag{8}$$

where $p_{R_1\,R_2}(x, y)$ is the joint PDF (JPDF) of the envelopes $R_1(t)$ and $R_2(t)$. Owing again to the independence assumption, this JPDF can be written as the product of the two marginal PDFs $p_{R_1}(x)$ and $p_{R_2}(y)$, i.e., $p_{R_1\,R_2}(x, y) = p_{R_1}(x)\, p_{R_2}(y)$. Hence, the PDF of the double Hoyt process $R(t)$ is given by

$$p_R(z) = \frac{\sqrt{A_{q_1} A_{q_2}}}{\Omega_1 \Omega_2} z \int_0^{\infty} \frac{1}{y} \exp\left[-\frac{A_{q_1} z^2}{4\Omega_1 y^2} - \frac{A_{q_2} y^2}{4\Omega_2}\right] \times I_0\left(\frac{B_{q_1}}{4\Omega_1}\frac{z^2}{y^2}\right) I_0\left(\frac{B_{q_2}}{4\Omega_2} y^2\right) dy \tag{9}$$

where $A_{q_i} = \left((1+q_i^2)/q_i\right)^2$ and $B_{q_i} = (1-q_i^4)/q_i^2$ $(i = 1, 2)$. As a key step towards solving the integral in (9), we employ the integral form of the Bessel function $I_0(z) = \frac{1}{\pi}\int_0^{\pi} \exp(z\cos(\theta))\, d\theta$ (see [38, eq. (8.431.3)]), which yields

$$p_R(z) = \frac{\sqrt{A_{q_1} A_{q_2}}}{\pi^2 \Omega_1 \Omega_2} z \int_0^{\pi}\int_0^{\pi} d\theta_1 d\theta_2 \int_0^{\infty} \frac{1}{y} \times \exp\left[\frac{-(A_{q_1} - B_{q_1}\cos(\theta_1))}{4\Omega_1}\frac{z^2}{y^2}\right] \times \exp\left[\frac{-(A_{q_2} - B_{q_2}\cos(\theta_2))}{4\Omega_2} y^2\right] dy. \tag{10}$$

Then, by making the change of variable $x = y^2$ and using [38, eq. (3.471.9)], it is possible to carry out the semi-infinite integral in (10) explicitly to obtain the following PDF of double Hoyt processes $R(t)$

$$p_R(z) = \frac{\sqrt{A_{q_1} A_{q_2}}}{\pi^2 \Omega_1 \Omega_2} z \int_0^{\pi}\int_0^{\pi} d\theta_1 d\theta_2 K_0\left(\frac{z}{2\sqrt{\Omega_1\Omega_2}}\sqrt{(A_{q_1} - B_{q_1}\cos(\theta_1))(A_{q_2} - B_{q_2}\cos(\theta_2))}\right). \tag{11}$$

It can be observed that the provided solution for the semi-infinite range integral in (9) could be replaced by a double-integral of trigonometric functions with finite limits. To the best of the authors' knowledge, the PDF in (11) is new and more computationally tractable than the equivalent single semi-infinite range integral representation in (9). In addition, (11) is more suitable for insightful analytical investigations, e.g., the SEP performance analysis as will be shown in Section IV. For the special case of Hoyt×Rayleigh fading, obtained by setting $q_2 = 1$ in the expressions for $A_{q_2}$ and $B_{q_2}$, the integral with respect to the variable $\theta_2$ can be carried out, and (11) simplifies to

$$p_R(z) = \frac{2\sqrt{A_{q_1}}}{\pi \Omega_1 \Omega_2} z \times \int_0^{\pi} K_0\left(\frac{z}{\sqrt{\Omega_1\Omega_2}}\sqrt{(A_{q_1} - B_{q_1}\cos(\theta_1))}\right) d\theta_1. \tag{12}$$

Here, it goes without saying that a distribution having the same functional form as (12) can be obtained by inserting $q_1 = 1$ in the quantities $A_{q_1}$ and $B_{q_1}$ appearing in (11) and performing the integration with respect to the variable $\theta_1$. Similarly, for the trivial case of double Rayleigh fading, where $q_i = 1$ in $A_{q_i}$ and $B_{q_i}$ $(i = 1, 2)$, the double-finite range integral in (11) can be solved analytically to yield the already known closed-form expression for the PDF $p_R(z)$ [7]. For completeness, we should add that the derived PDF $p_R(z)$ in (11) also incorporates the limiting cases known as Hoyt×one-sided Gaussian ($q_2 \to 0$), Rayleigh×one-sided Gaussian ($q_1 = 1, q_2 \to 0$), and double one-sided Gaussian ($q_1 \to 0$, $q_2 \to 0$) distributions. Unfortunately, the determination of these limiting PDFs from (11) has been found to be tedious. Instead, we may seek to provide formulas for the underlying PDFs by making use of the involved distributions and applying the concept of transformation of random variables described in (8). Accomplishing this task, we obtain closed-form expressions for the PDFs of the envelope in cascaded Rayleigh×one-sided Gaussian and double one-sided Gaussian fading channels as

$$p_R(z) = \sqrt{\frac{2}{\Omega_1\Omega_2}} z \exp\left[-\sqrt{\frac{2}{\Omega_1\Omega_2}} z\right] \tag{13}$$

$$p_R(z) = \frac{2}{\pi\sqrt{\Omega_1\Omega_2}} K_0\left(\frac{z}{\sqrt{\Omega_1\Omega_2}}\right) \tag{14}$$

respectively. It should be mentioned that (13) and (14) have been derived using [38, eq. (3.472.3)] and [38, eq. (3.471.9)], respectively. Unfortunately, a simplified expression for the PDF of the cascaded Hoyt×one-sided Gaussian channel does not exist.

Using the PDF derived above, we can readily determine the CDF $F_R(z)$ of double Hoyt processes $R(t)$. This statistical quantity is obtained according to [37]

$$F_R(z) = \int_0^z p_R(x) dx. \tag{15}$$

Substituting (11) in (15), letting $y = (x/z)$, and using [38, eqs. (6.561.8) and (2.553.3)], an expression for the CDF $F_R(z)$ is given by

$$F_R(z) = 1 - \frac{2}{\pi^2}\sqrt{\frac{A_{q_1} A_{q_2}}{\Omega_1\Omega_2}} z \int_0^{\pi}\int_0^{\pi} d\theta_1 d\theta_2 \times \frac{K_1\left(\frac{z}{2\sqrt{\Omega_1\Omega_2}}\sqrt{(A_{q_1} - B_{q_1}\cos(\theta_1))(A_{q_2} - B_{q_2}\cos(\theta_2))}\right)}{\sqrt{(A_{q_1} - B_{q_1}\cos(\theta_1))(A_{q_2} - B_{q_2}\cos(\theta_2))}} \tag{16}$$

where $K_1(\cdot)$ stands for the first-order modified Bessel function of the second kind [38]. Setting $q_2 = 1$ in (16), the finite-range integral with respect to the variable $\theta_2$ can be solved, yielding the following expression for the CDF of cascaded Hoyt×Rayleigh fading channels

$$F_R(z) = 1 - \frac{2}{\pi}\sqrt{\frac{A_{q_1}}{\Omega_1\Omega_2}}z\int_0^{\pi}\frac{1}{\sqrt{(A_{q_1} - B_{q_1}\cos(\theta_1))}} \times K_1\left(\frac{z}{\sqrt{\Omega_1\Omega_2}}\sqrt{(A_{q_1} - B_{q_1}\cos(\theta_1))}\right)d\theta_1. \quad (17)$$

By setting $q_1 = 1$ in (17), it can be verified that the CDF reduces to that of double Rayleigh fading channels [7]. In the same way, the CDF of the Rayleigh×one-sided Gaussian fading envelope can be obtained using (13) and with the help of [38, eq. (2.322)] as

$$F_R(z) = \sqrt{\frac{\Omega_1\Omega_2}{2}} - \left(z + \sqrt{\frac{\Omega_1\Omega_2}{2}}\right)\exp\left(-\sqrt{\frac{2}{\Omega_1\Omega_2}}z\right). \quad (18)$$

To conclude this section, we point out that the outage probability $P_{out}(r)$ of the end-to-end radio links is defined as the probability that the process $R(t)$ falls below a threshold value $r$, which means that this performance metric equals the CDF $F_R(z)$ of $R(t)$, i.e., $P_{out}(r) = F_R(r)$.

## III. LCR AND ADF OF THE ENVELOPE FADING PROCESS *R(t)*

To have a thorough knowledge of the statistics of double Hoyt fading channels, it is also common to investigate the corresponding LCR and ADF quantities. Expressions for these quantities will be derived in the sequel.

### A. Exact Theoretical Solution for the LCR

The LCR describes how often the process $R(t)$ crosses a given level $r$ from up to down (or from down to up) per time unit. This statistical quantity, denoted here by $N_R(r)$, can be obtained by solving the following integral [40], [41]

$$N_R(r) = \int_0^{\infty}\dot{z}\,p_{R\dot{R}}(r,\dot{z})\,d\dot{z} \quad (19)$$

where $p_{R\dot{R}}(z,\dot{z})$ is the JPDF of the double Hoyt process $R(t)$ and its time derivative $\dot{R}(t)$ at the same time instant. Owing to the fact that the processes $R_1(t)$ and $R_2(t)$ are mutually independent, the JPDF $p_{R\dot{R}}(z,\dot{z})$ can be obtained by invoking the standard result in [42] as

$$p_{R\dot{R}}(z,\dot{z}) = \int_0^{\infty}\int_{-\infty}^{\infty}\frac{1}{y^2}p_{R_1\dot{R}_1}\left(\frac{z}{y},\frac{\dot{z}}{y} - \frac{z}{y^2}\dot{y}\right) \times p_{R_2\dot{R}_2}(y,\dot{y})\,d\dot{y}dy \quad z \geq 0, \quad |\dot{z}| < \infty \quad (20)$$

where $p_{R_i\dot{R}_i}(x,\dot{x})$ $(i = 1,2)$ represents the JPDF of the Hoyt process $R_i(t)$ and its time derivative $\dot{R}_i(t)$, which is given by [27]

$$p_{R_i\dot{R}_i}(x,\dot{x}) = \frac{\sqrt{A_{q_i}}}{\sqrt{2}\pi^{3/2}\Omega_i}x\int_0^{\pi}\frac{1}{\sqrt{\left(\beta_{Y_i} + \left(\beta_{X_i} - \beta_{Y_i}\right)\cos^2(\theta)\right)}} \times\exp\left[-\frac{\sqrt{A_{q_i}}}{2\Omega_i}x^2\left(q_i^2\cos^2(\theta) + \sin^2(\theta)\right)\right] \times\exp\left[-\frac{\dot{x}^2}{2\left(\beta_{Y_i} + \left(\beta_{X_i} - \beta_{Y_i}\right)\cos^2(\theta)\right)}\right]d\theta \quad (21)$$

where the quantities $\beta_{X_i}$ and $\beta_{Y_i}$ represent the negative curvature of the autocorrelation functions $\Gamma_{X_iX_i}(\tau)$ and $\Gamma_{Y_iY_i}(\tau)$ of the processes $X_i(t)$ and $Y_i(t)$, respectively, at $\tau = 0$, i.e., $\beta_{X_i} = -\ddot{\Gamma}_{X_iX_i}(0)$ and $\beta_{Y_i} = -\ddot{\Gamma}_{Y_iY_i}(0)$. Now, by substituting (21) in (20) and with the help of [38, eq. (3.323.2[7])], we get the following expression for the JPDF $p_{R\dot{R}}(z,\dot{z})$ of the processes $R(t)$ and $\dot{R}(t)$

$$p_{R\dot{R}}(z,\dot{z}) = \frac{\sqrt{A_{q_1}A_{q_2}}}{\sqrt{2}\pi^{5/2}\Omega_1\Omega_2}z\int_0^{\pi}d\theta_1\int_0^{\pi}d\theta_2\int_0^{\infty}dy \frac{1}{\sqrt{z^2F(\theta_2) + y^4F(\theta_1)}}\exp\left[-\frac{\sqrt{A_{q_1}}}{2q_1\Omega_1}\frac{z^2}{y^2}G(\theta_1)\right] \times\exp\left[-\frac{\sqrt{A_{q_2}}}{2q_2\Omega_2}y^2G(\theta_2)\right] \times\exp\left[-\frac{(\dot{z}y)^2}{2\left[z^2F(\theta_2) + y^4F(\theta_1)\right]}\right] \quad (22)$$

where the functions $F(\theta_i)$ and $G(\theta_i)$ $(i = 1,2)$ are given by

$$F(\theta_i) = \beta_{Y_i} + \left(\beta_{X_i} - \beta_{Y_i}\right)\cos^2(\theta_i)$$
$$G(\theta_i) = q_i^2\cos^2(\theta_i) + \sin^2(\theta_i). \quad (23)$$

Finally, after substituting (22) in (19) and performing again some algebraic manipulations, the LCR $N_R(r)$ of the double Hoyt fading process $R(t)$ can be expressed in the final form as

$$N_R(r) = \frac{\sqrt{A_{q_1}A_{q_2}}}{\sqrt{2}\pi^{5/2}\Omega_1\Omega_2}r\int_0^{\pi}d\theta_1\int_0^{\pi}d\theta_2\int_0^{\infty}\frac{1}{y} \times\sqrt{\left(\frac{r}{y}\right)^2F(\theta_2) + y^2F(\theta_1)} \times\exp\left[-\left(\frac{\sqrt{A_{q_1}}}{2q_1\Omega_1}\left(\frac{r}{y}\right)^2G(\theta_1) + \frac{\sqrt{A_{q_2}}}{2q_2\Omega_2}y^2G(\theta_2)\right)\right]dy. \quad (24)$$

Unfortunately, the integrals appearing in (24) do not have closed-form solutions, and thus need to be evaluated using numerical integration techniques. For the particular case of double Rayleigh channels, obtained by setting $q_1 = q_2 = 1$ in (24), the integration with respect to $\theta_1$ and $\theta_2$ becomes possible, and (24) reduces to the known semi-infinite range

integral expression reported in [13, eq. (17)]. That is, even for the particular case of double Rayleigh fading channels reported in [13], the semi-infinite range integral in (24) cannot be solved. To reduce the computational effort, we provide next an approximate expression for the LCR of the double Hoyt fading process by using Laplace's approximation theorem [35].

### B. Approximate Theoretical Solution for the LCR

Since a closed-form solution does not exist for the inner-integral in (24), it is desirable to find at least an approximate solution. As outlined in Appendix A, the approximation of the semi-infinite range integral in (24) using Laplace's approximation theorem [35] leads to the following result for the LCR $N_R(r)$ of the process $R(t)$

$$N_R(r) \approx \frac{\sqrt{A_{q_1}A_{q_2}}}{2\pi^2\Omega_1\Omega_2} r \int_0^{\pi}\int_0^{\pi} \sqrt{\frac{q_1\Omega_1 F(\theta_2)}{\sqrt{A_{q_1}}G(\theta_1)} + \frac{q_2\Omega_2 F(\theta_1)}{\sqrt{A_{q_2}}G(\theta_2)}} \times \exp\left(-\frac{(A_{q_1}A_{q_2})^{\frac{1}{4}}}{\sqrt{\Omega_1\Omega_2}}\sqrt{\frac{G(\theta_1)G(\theta_2)}{q_1 q_2}}r\right) d\theta_1 d\theta_2. \tag{25}$$

For the special case that the envelope $R(t)$ is Hoyt×Rayleigh distributed, i.e., $q_2 = 1$, (25) reduces to

$$N_R(r) \approx \frac{\sqrt{A_{q_1}}}{\pi\Omega_1\Omega_2} r \int_0^{\pi} \sqrt{\frac{q_1\Omega_1\beta_{Y_2}}{\sqrt{A_{q_1}}G(\theta_1)} + \frac{\Omega_2 F(\theta_1)}{2}} \times \exp\left(-\frac{\sqrt{2}\,(A_{q_1})^{\frac{1}{4}}}{\sqrt{\Omega_1\Omega_2}}\sqrt{\frac{G(\theta_1)}{q_1}}r\right) d\theta_1. \tag{26}$$

If in addition $q_1 = 1$, then (26) results in the already known approximate solution for the LCR of double Rayleigh processes, which was derived in [19, eq. (33)].

### C. ADF $T_R(r)$ of the Double Hoyt Process $R(t)$

In addition to the LCR, the ADF is of great importance to the characterization of fading channels. The ADF $T_R(r)$ of the double Hoyt processes $R(t)$ is the expected value of the length of the time intervals during which the process $R(t)$ is below a given level $r$. Following [43], the ADF $T_R(r)$ of the double Hoyt process $R(t)$ is defined by

$$T_R(r) = \frac{F_R(r)}{N_R(r)}. \tag{27}$$

By substituting (16) and (24) in (27), a formula for the ADF $T_R(r)$ of the double Hoyt process $R(t)$ can be deduced. Furthermore, by substituting the obtained approximate solution for the LCR $N_R(r)$ according to (25) in (27), we obtain an approximate expression for the ADF $T_R(r)$.

Apart from the outage based performance metrics derived above, the average SEP is a common performance metric in wireless communications. In the next section, analytical expressions are derived for the SEP performance of coherent M-PSK and square M-QAM modulation schemes.

## IV. SEP OF M-PSK AND M-QAM MODULATION SCHEMES

We assume that the double Hoyt channel fading is slow and frequency non-selective. The derivation of the SEP of coherent M-PSK and square M-QAM modulation schemes is carried out by invoking the conventional PDF approach [30]. According to this approach, the corresponding SEP can be obtained by solving the following integral

$$\bar{P}_s = \int_0^{\infty} P_s(E|\gamma) p_\gamma(\gamma)\, d\gamma \tag{28}$$

where $P_s(E|\gamma)$ denotes the conditional SEP in additive white Gaussian noise channels, and $p_\gamma(\gamma)$ stands for the PDF of the instantaneous SNR per symbol $\gamma(t) = R^2(t)\left(E_s/N_0\right)$, with $E_s$ being the average received symbol energy, and $N_0$ the one-sided power spectral density of the receiver noise. The PDF $p_\gamma(\gamma)$ of $\gamma(t)$ can directly be obtained from the PDF $p_R(z)$ of the envelope $R(t)$ by using [30, eq. (2.3)]. As a result, it follows that

$$p_\gamma(\gamma) = \frac{\sqrt{A_{q_1}A_{q_2}}}{2\pi^2\bar{\gamma}} \int_0^{\pi}\int_0^{\pi} d\theta_1 d\theta_2 \, K_0\left(\frac{1}{2}\sqrt{\frac{\gamma}{\bar{\gamma}}}\sqrt{\left(A_{q_1} - B_{q_1}\cos(\theta_1)\right)\left(A_{q_2} - B_{q_2}\cos(\theta_2)\right)}\right) \tag{29}$$

where $\bar{\gamma} = \Omega_1\Omega_2\left(E_s|N_0\right)$ denotes the average SNR. Expressions for the SEP of M-PSK and M-QAM modulation schemes are thoroughly derived in the following subsections.

### A. SEP OF M-PSK MODULATION

For coherent M-PSK modulation, the conditional SEP $P_s(E|\gamma)$ is given by [30, eq. (8.23)]

$$P_s(E|\gamma) = \frac{1}{\pi}\int_0^{(M-1)\pi/M} \exp\left(-\frac{g_{psk}}{\sin^2(\varphi)}\gamma\right) d\varphi \tag{30}$$

where $g_{psk} = \sin^2(\pi/M)$, and $M$ is the number of possible transmitted information symbols. Substituting (29) and (30) in (28) and using [38, eqs. (6.614.4) and (8.338.1)] and [39, eq. (13.18.5)], the SEP $\bar{P}_s$ of M-PSK modulation is given by

$$\bar{P}_s = \frac{\sqrt{A_{q_1}A_{q_2}}}{4\pi^3 g_{psk}\bar{\gamma}} \int_0^{\pi} d\theta_1 \int_0^{\pi} d\theta_2 \int_0^{(M-1)\pi/M} \sin^2(\theta_3) d\theta_3 \times\Gamma\left(0, \frac{\sin^2(\theta_3)}{16 g_{psk}\bar{\gamma}}(A_{q_1} - B_{q_1}\cos(\theta_1))(A_{q_2} - B_{q_2}\cos(\theta_2))\right) \times \exp\left(\frac{\sin^2(\theta_3)}{16 g_{psk}\bar{\gamma}}(A_{q_1} - B_{q_1}\cos(\theta_1))(A_{q_2} - B_{q_2}\cos(\theta_2))\right) \tag{31}$$

where $\Gamma(\cdot,\cdot)$ denotes the incomplete gamma function defined in [39, eq. (8.4.4)]. The finite-range integrals in (31) can be efficiently computed using numerical integration techniques. For the special case of the asymmetrical

Hoyt×Rayleigh fading, i.e., $q_2 = 1$, the SEP $\bar{P}_s$ in (31) simplifies to

$$\bar{P}_s = \frac{\sqrt{A_{q_1}}}{2\pi^2 g_{psk}\bar{\gamma}} \int_0^{\pi} d\theta_1 \int_0^{(M-1)\pi/M} \sin^2(\theta_3) d\theta_3 \times \Gamma\left(0, \frac{\sin^2(\theta_3)}{4g_{psk}\bar{\gamma}}(A_{q_1} - B_{q_1}\cos(\theta_1))\right) \times \exp\left(\frac{\sin^2(\theta_3)}{4g_{psk}\bar{\gamma}}(A_{q_1} - B_{q_1}\cos(\theta_1))\right). \quad (32)$$

If in addition $q_1 = 1$, then the integral with respect to $\theta_1$ can be solved and we obtain the SEP $\bar{P}_s$ of double Rayleigh fading channels as

$$\bar{P}_s = \frac{1}{\pi g_{psk}\bar{\gamma}} \int_0^{(M-1)\pi/M} \sin^2(\theta_3) \exp\left(\frac{\sin^2(\theta_3)}{g_{psk}\bar{\gamma}}\right) \times \Gamma\left(0, \frac{\sin^2(\theta_3)}{g_{psk}\bar{\gamma}}\right) d\theta_3. \quad (33)$$

Letting $M = 2$ in (33) and using [39, eq. (13.18.5)], yields the bit error probability of binary PSK modulation reported in [44, eq. (17)].

For the special cases of Rayleigh×one-sided Gaussian and double one-sided Gaussian fading channels, the corresponding SEP of M-PSK can directly be determined using the PDFs given in (13) and (14), respectively. To proceed, we consider first the Rayleigh×one-sided Gaussian channel. Substituting $p_\gamma(\gamma)$ deduced from (13) together with (30) into (28) and using [38, eqs. (3.333.2), (8.25.1), and (8.25.4)] yields

$$\bar{P}_s = \frac{1}{\sqrt{2\pi g_{psk}\bar{\gamma}}} \int_0^{(M-1)\pi/M} \sin(\theta) \exp\left(\frac{\sin^2(\theta)}{2g_{psk}\bar{\gamma}}\right) \times erfc\left(\frac{\sin(\theta)}{\sqrt{2g_{psk}\bar{\gamma}}}\right) d\theta \quad (34)$$

where $erfc(\cdot)$ represents the complementary error function [38]. Similarly, substituting the expression of $p_\gamma(\gamma)$, obtained from (14), and (30) in (28), results, after some algebraic manipulations, in the following expression for the SEP of M-PSK over double one-sided Gaussian channels

$$\bar{P}_s = \frac{1}{2\pi^{3/2}\sqrt{g_{psk}\bar{\gamma}}} \int_0^{(M-1)\pi/M} \sin(\theta) \exp\left(\frac{\sin^2(\theta)}{8g_{psk}\bar{\gamma}}\right) \times K_0\left(\frac{\sin^2(\theta)}{8g_{psk}\bar{\gamma}}\right) d\theta. \quad (35)$$

### B. SEP OF SQUARE M-QAM MODULATION

In the case of M-QAM modulation with square signal constellation diagrams, the conditional SEP $P_s(E|\gamma)$ is given by [30, eq. (9.20)]

$$P_s(E|\gamma) = 4\left(1 - \frac{1}{\sqrt{M}}\right) Q\left(\sqrt{2g_{QAM}\gamma}\right) - 4\left(1 - \frac{1}{\sqrt{M}}\right)^2 Q^2\left(\sqrt{2g_{QAM}\gamma}\right) \quad (36)$$

where $g_{QAM} = 3/(2(M-1))$, and $Q(\cdot)$ represents the Gaussian $Q$-function [30, eq. (4.2)]. Substituting (29) and (36) in (28), and performing the algebraic manipulations explained in Appendix B, the average SEP $\bar{P}_s$ of square M-QAM modulation over double Hoyt fading channels is obtained as

$$\bar{P}_s = f_1\left(4\left(1 - \frac{1}{\sqrt{M}}\right), \frac{\pi}{2}\right) - f_1\left(4\left(1 - \frac{1}{\sqrt{M}}\right)^2, \frac{\pi}{4}\right) \quad (37)$$

where the function $f_1(\cdot,\cdot)$ is given by

$$f_1(a,\alpha) = \frac{a\sqrt{A_{q_1}A_{q_2}}}{4\pi^3 g_{QAM}\bar{\gamma}} \int_0^{\pi} d\theta_1 \int_0^{\pi} d\theta_2 \int_0^{\alpha} \sin^2(\theta_3) d\theta_3 \times \Gamma\left(0, \frac{\sin^2(\theta_3)}{16g_{QAM}\bar{\gamma}}(A_{q_1} - B_{q_1}\cos(\theta_1))(A_{q_2} - B_{q_2}\cos(\theta_2))\right) \times \exp\left(\frac{\sin^2(\theta_3)}{16g_{QAM}\bar{\gamma}}(A_{q_1} - B_{q_1}\cos(\theta_1))(A_{q_2} - B_{q_2}\cos(\theta_2))\right). \quad (38)$$

For Hoyt×Rayleigh fading scenarios, where $q_2 = 1$, (37) simplifies to

$$\bar{P}_s = f_2\left(4\left(1 - \frac{1}{\sqrt{M}}\right), \frac{\pi}{2}\right) - f_2\left(4\left(1 - \frac{1}{\sqrt{M}}\right)^2, \frac{\pi}{4}\right) \quad (39)$$

where

$$f_2(a,\alpha) = \frac{a\sqrt{A_{q_1}}}{2\pi^2 g_{QAM}\bar{\gamma}} \int_0^{\pi} d\theta_1 \int_0^{\alpha} \sin^2(\theta_3) \times \Gamma\left(0, \frac{\sin^2(\theta_3)}{4g_{QAM}\bar{\gamma}}(A_{q_1} - B_{q_1}\cos(\theta_1))\right) \times \exp\left(\frac{\sin^2(\theta_3)}{4g_{QAM}\bar{\gamma}}(A_{q_1} - B_{q_1}\cos(\theta_1))\right) d\theta_3. \quad (40)$$

Furthermore, the corresponding results for double Rayleigh fading channels are obtained by setting $q_1 = 1$ in (39), which results in the following expression for the SEP

$$\bar{P}_s = \frac{4}{\pi g_{QAM}\bar{\gamma}}\left(1 - \frac{1}{\sqrt{M}}\right) \int_0^{\pi/2} \sin^2(\theta_3)\Gamma\left(0, \frac{\sin^2(\theta_3)}{g_{QAM}\bar{\gamma}}\right) \times \exp\left(\frac{\sin^2(\theta_3)}{g_{QAM}\bar{\gamma}}\right) d\theta_3 - \frac{4}{\pi g_{QAM}\bar{\gamma}}\left(1 - \frac{1}{\sqrt{M}}\right)^2 \int_0^{\pi/4} \sin^2(\theta_3)\Gamma\left(0, \frac{\sin^2(\theta_3)}{g_{QAM}\bar{\gamma}}\right) \times \exp\left(\frac{\sin^2(\theta_3)}{g_{QAM}\bar{\gamma}}\right) d\theta_3. \quad (41)$$

**TABLE 1.** The optimized parameters of the analytical double Hoyt and double Rayleigh fading channel models for the highway propagation conditions.

| Optimized parameters | | | | | | | | | |
|---|---|---|---|---|---|---|---|---|---|
| Double Hoyt | | | | | | Double Rayleigh | | | |
| $q_1$ | $q_2$ | $\Omega_1$ | $\Omega_2$ | $f_{T,\max}$ | $f_{R,\max}$ | $\Omega_1$ | $\Omega_2$ | $f_{T,\max}$ | $f_{R,\max}$ |
| 0.8704 | 0.9638 | 1.4567 | 2.317 | 255.1942 | 55.9692 | 0.2207 | 13.3798 | 251.2249 | 88.7008 |

By proceeding similarly as in the case of M-PSK modulation, the SEP $\bar{P}_s$ over Rayleigh×one-sided Gaussian channels equals

$$\bar{P}_s = g_1\left(4\left(1-\frac{1}{\sqrt{M}}\right),\frac{\pi}{2}\right)-g_1\left(4\left(1-\frac{1}{\sqrt{M}}\right)^2,\frac{\pi}{4}\right) \tag{42}$$

where

$$g_1(a,\alpha) = \frac{a}{\sqrt{2\pi g_{QAM}\bar{\gamma}}}\int_0^{\alpha}\sin(\theta)\exp\left(\frac{\sin^2(\theta)}{2g_{QAM}\bar{\gamma}}\right) \times erfc\left(\frac{\sin(\theta)}{\sqrt{2g_{QAM}\bar{\gamma}}}\right)d\theta. \tag{43}$$

It should be mentioned that (42) was attained by using [38, eqs. (3.333.2), (8.25.1), and (8.25.4)] in combination with the alternate definite integral form of the Gaussian Q-function [30, eq. (4.2)] and its square [30, eq. (4.9)]. Finally, the SEP $\bar{P}_s$ of square M-QAM over double one-sided Gaussian channels, is determined by performing the required substitutions in (28) and using [30, eqs. (4.2) and (4.9)] and [38, eqs. (6.618.3), (1.411.9), and (9.72)]. This yields

$$\bar{P}_s = g_2\left(4\left(1-\tfrac{1}{\sqrt{M}}\right),\tfrac{\pi}{2}\right)-g_2\left(4\left(1-\tfrac{1}{\sqrt{M}}\right)^2,\tfrac{\pi}{4}\right) \tag{44}$$

where the function $g_2(\cdot,\cdot)$ has the form

$$g_2(a,\alpha) = \frac{a}{2\pi^{3/2}\sqrt{g_{QAM}\bar{\gamma}}}\int_0^{\alpha}\sin(\theta)\exp\left(\frac{\sin^2(\theta)}{8g_{QAM}\bar{\gamma}}\right) \times K_0\left(\frac{\sin^2(\theta)}{8g_{QAM}\bar{\gamma}}\right)d\theta. \tag{45}$$

## V. MODEL VALIDATION AND RESULTS VERIFICATION

In this section, we first check the validity of the double Hoyt distribution in describing real-word fading channels. We then present numerical and simulation results to verify the correctness of the derived statistical quantities.

### A. MODEL VALIDATION THROUGH MEASURED CHANNELS

For the validation of the proposed double Hoyt channel model, it is important to match its statistical properties against channel measurement data. Since double scattering is a typical propagation effect in V2V channels, where the scattering is supposed to occur around both the transmitter and the receiver, it is imperative in this study to corroborate the double Hoyt model with field measurements in V2V channels. To this end, we restrict our focus on the CDF and LCR of the fading envelope and use the corresponding measurements of inter-vehicular communication channels available in [8]. These measurements were collected at 5.2 GHz in highway environment. The set of channel parameters controlling the CDF and LCR is restricted to $q_1$, $q_2$, $\Omega_1$, $\Omega_2$, $f_{T,\max}$, and $f_{R,\max}$, in which $f_{T,\max}$ and $f_{R,\max}$ stand for the maximum Doppler frequencies experienced at the mobile transmitter and the mobile receiver, respectively. To examine the suitability of the model, these parameters have to be optimized by applying standard optimization procedures aiming to minimize the deviations between the analytical and measured CDFs and LCRs of V2V channels. Performing the numerical optimization resulted in the optimized model parameters values shown in Table 1 for the highway propagation scenario. Making use of these values, the CDF and LCR of the double Hoyt model are obtained and compared with corresponding measurements. Fig. 1 depicts the optimized CDF together with the measured CDF reproduced from [8]. The optimized CDF of a double Rayleigh fading process is also shown for comparison. The conclusion to be drawn from this figure is that the fading occurring on the real-world V2V channel is seen to be worse than the one predicted by the double Rayleigh model, and appears to be closely described by the double Hoyt model. This observation demonstrates the flexibility and potential of the double Hoyt model in

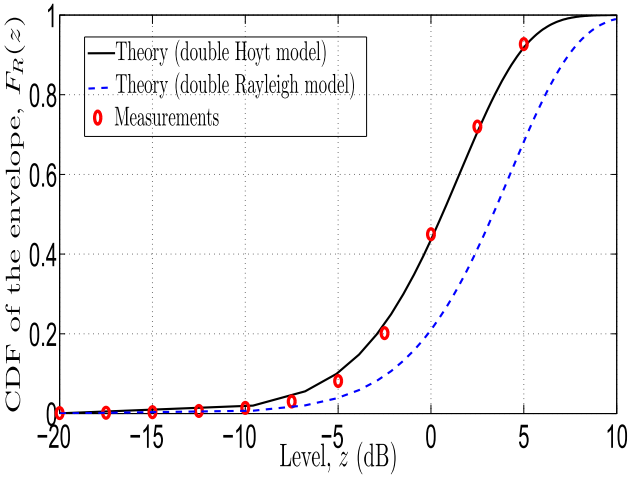


**FIGURE 1.** The optimized CDF $F_R(z)$ of the double Hoyt and double Rayleigh processes for the highway propagation conditions.

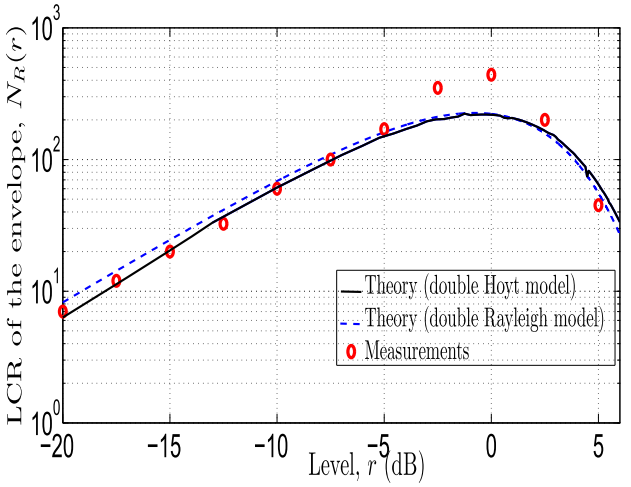


**FIGURE 2.** The optimized LCR $N_R(r)$ of the double Hoyt and double Rayleigh processes for the highway propagation conditions.

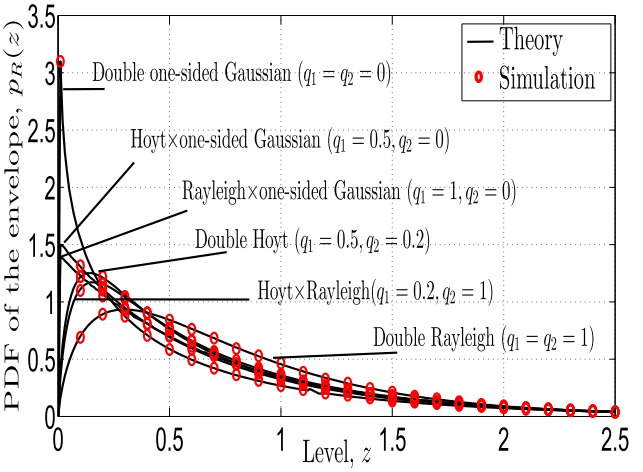


**FIGURE 3.** The envelope PDF $p_R(z)$ of the double Hoyt process $R(t)$ for different combinations of the Hoyt fading parameters $q_1$ and $q_2$.

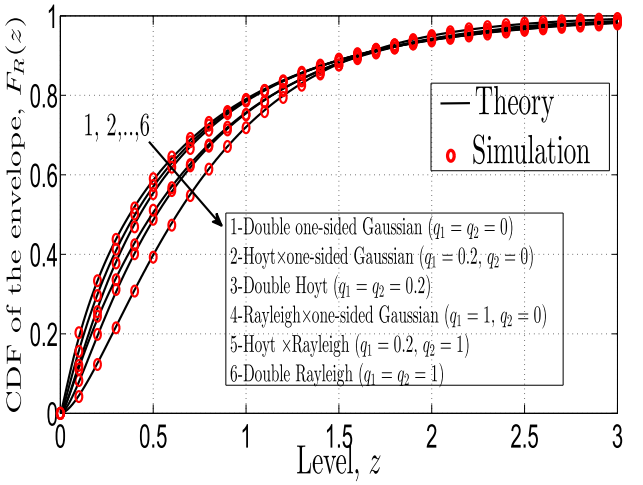


**FIGURE 4.** The CDF $F_R(z)$ of the double Hoyt process $R(t)$ for different combinations of the Hoyt fading parameters $q_1$ and $q_2$.

describing severe multipath fading scenarios. Next, the comparison between the measured LCR of the considered real-word V2V channel [8] and the LCRs predicted by the double Rayleigh and double Hoyt channels is shown in Fig. 2. It is apparent that both models are useful to describe the measured data especially in the low amplitude regime, although the double Hoyt model produces a slightly better match. Overall, these preliminary observations reveal that, due to its enough flexibility, the double Hoyt distribution has the potential to be applicable in the description of realistic V2V fading channels, where the propagation conditions are more severe than those described by the double Rayleigh model. To the best of our knowledge, not a single previous study considered the applicability of the double Hoyt multipath propagation model in the description of realistic inter-vehicular fading channels. We believe that the study of double or, in general, multiple scattering effects requires further extensive field measurements.

### *B. NUMERICAL AND SIMULATION RESULTS*

In this section, numerical and simulation results are provided to check the validity of the theoretical results and to visualize the impact of double Hoyt fading on the performance of wireless V2V communication systems. We assume the widely adopted Clarke's 2-D channel model for the scattering environment. The concept of Rice's sum-of-sinusoids [40], [41] has been adopted to perform the simulations, and the method of exact Doppler spread [42] has been employed to determine the parameters of the sinusoids. For the fading conditions described above, the second spectral moments $\beta_{X_i}$ $(i = 1, 2)$ of the processes $X_i(t)$ are given by $\beta_{X_1} = \frac{2}{1+q_1^2}\Omega_1 \left(\pi f_{T,\max}\right)^2$ and $\beta_{X_2} = \frac{2}{1+q_2^2}\Omega_2 \left(\pi f_{R,\max}\right)^2$ [43] whereas $\beta_{Y_i} = q_i^2\beta_{X_i}$. All results presented here are obtained for $\Omega_1 = \Omega_2 = 1$, $f_{T,\max} = 20$ Hz, and $f_{R,\max} = 30$ Hz. As can be observed, the theoretical and simulation results are in perfect agreement demonstrating the correctness of the derivations. Fig. 3 shows the theoretical and simulated PDF $p_R(z)$ of the double Hoyt process $R(t)$ for different combinations of the Hoyt fading parameters $q_1$ and $q_2$. As can be noted, the location of the peak of the PDF is shifted to the left with decreasing values of the Hoyt fading parameters, illustrating the fact that the fading severity increases with decreasing values of $q_1$ and $q_2$. Fig. 4 illustrates the behavior of the CDF $F_R(r)$ (or equivalently the outage probability) of double Hoyt, double Rayleigh, double one-sided Gaussian, Hoyt×one-sided Gaussian, Rayleigh×one-sided Gaussian, and Hoyt×Rayleigh fading channels. Note that the outage performance improves with increasing values of $q_1$ and $q_2$, as was to be expected. In Fig. 5, we compare the exact theoretical, simulated, and approximate LCR $N_R(r)$ of the double Hoyt process $R(t)$ for various values of the Hoyt fading parameters $q_1$ and $q_2$ with $q_1 = q_2$. For this low mobility scenario, where $f_{T,\max} = 20$ Hz and $f_{R,\max} = 30$

**TABLE 2.** Mean square error for $q_1 = 0.5$, $q_2 = 0.5$, $f_{R,\max} = 30$ Hz, and different values of the maximum Doppler frequency $f_{T,\max}$.

| $f_{T,\max}$ | 50 | 80 | 120 | 170 | 200 | 250 | 500 |
|---|---|---|---|---|---|---|---|
| MSE | 1.6413 | 1.4906 | 1.1088 | 0.7664 | 0.6279 | 0.4682 | 0.1852 |

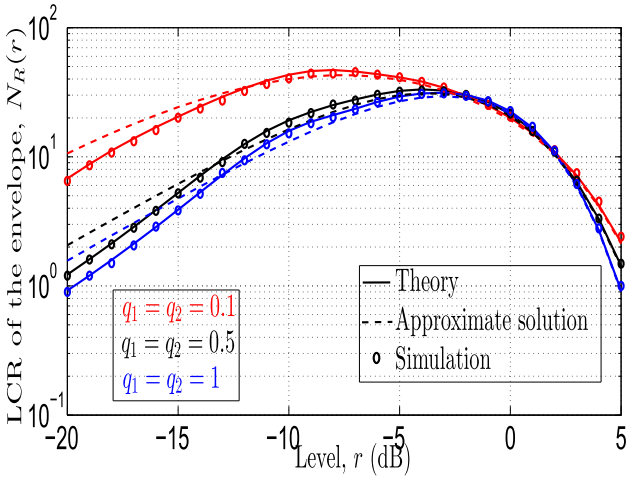


**FIGURE 5.** The LCR $N_R(r)$ of the double Hoyt process $R(t)$ for various values of the Hoyt fading parameters $q_1$ and $q_2$.

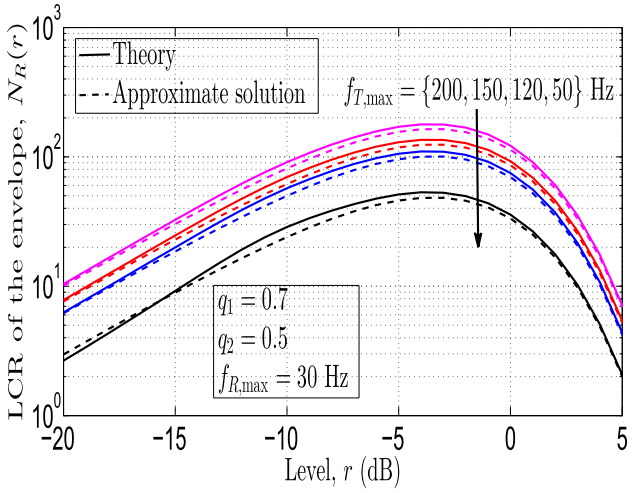


**FIGURE 6.** The LCR $N_R(r)$ of the double Hoyt process $R(t)$ for different values of the maximum Doppler frequency $f_{T,\max}$.

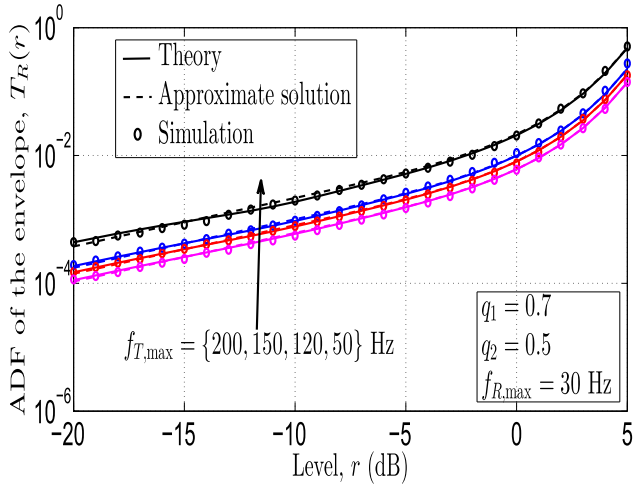


**FIGURE 7.** The ADF $T_R(r)$ of the double Hoyt process $R(t)$ for different values of the maximum Doppler frequency $f_{T,\max}$.

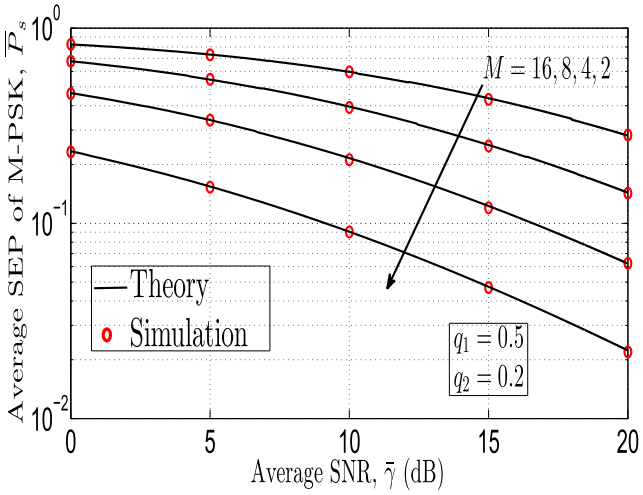


**FIGURE 8.** The SEP $\bar{P}_s$ of coherent M-PSK modulation schemes over double Hoyt fading channels.

Hz, the approximate result is seen to slightly deviate from the exact solution. In contrast, this deviation tends to disappear with increasing values of the Doppler frequencies as can be noted from the content of Fig. 6. This numerical observation reveals that the LCR approximation is computationally advantageous for the case of moderate and high Doppler frequencies. The same finding can also be noted for the ADF results reported in Fig. 7. In this figure, the exact theoretical, simulated, and approximate ADF $T_R(r)$ are seen to be in good correspondence for high values of the maximum Doppler frequency $f_{T,\max}$. To provide an accuracy assessment of the approximation, the mean square error (MSE) between the approximate and exact LCR solutions is computed. The obtained results are reported in Table 2, from which it is observed that the MSE declines as the Doppler frequency increases. Fig. 8 illustrates the SEP of M-PSK over double Hoyt fading channels for different values of $M \in \{2, 4, 8, 16\}$. As expected, by increasing $M$, the quality of the transmission deteriorates and the SEP increases. Finally, the SEP of 4-QAM is sketched in Fig. 9 to demonstrate the effect of the fading severity parameters $q_1$ and $q_2$. It can be noticed that an increase in the values of these parameters yields an improvement in the SEP performance. Namely, the best SEP performance of 4-QAM is obtained in double

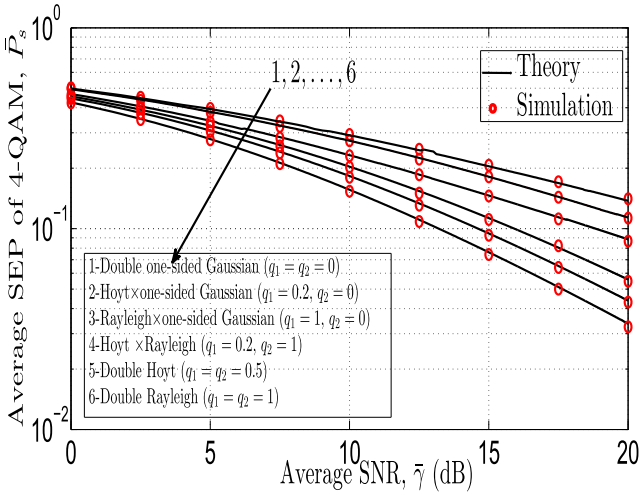


**FIGURE 9.** The SEP $\bar{P}_s$ of 4-QAM modulation schemes over double Hoyt fading channels.

Rayleigh fading channels, while the worst one corresponds to the case of double one-sided Gaussian fading channels.

## VI. CONCLUSION

In this paper, the statistical properties of double Hoyt fading channels have been analyzed. Analytical expressions have been derived for the PDF of the quadrature components of the overall complex channel gain as well as for the PDF and CDF of the envelope process. In addition, exact and approximate analytical solutions for the LCR and ADF of double Hoyt fading processes have been determined. Moreover, the SEP performance of M-PSK and square M-QAM modulation schemes over double Hoyt fading channels has been studied. Explicit formulas for the above metrics have been presented for channels that are special cases of the double Hoyt fading model. To examine the capability of the underlying channel model to describe real-word channels, the derived CDF and LCR of the double Hoyt channel model have been matched to those of published measured CDF and LCR of V2V channels. It has been observed that the envelope statistics of the double Hoyt model are in close agreement with the corresponding measured statistics, demonstrating its potential to statistically describe realistic inter-vehicular propagation scenarios. Finally, all the derived analytical results have been verified by means of computer simulations.

## APPENDIX A

In this Appendix, we outline the steps taken in the derivation of the approximate solution in (25) for the LCR $N_R(r)$ of the double Hoyt process $R(t)$. The employed Laplace approximation theorem is based on the following Laplace-type integral [35]

$$J(\lambda) = \int_0^\infty g(y)\exp\left(-\lambda f(y)\right)dy \simeq \sqrt{\frac{2\pi}{\lambda}}\cdot\frac{g(y_0)}{\sqrt{\ddot{f}(y_0)}}\exp\left(-\lambda f(y_0)\right) \quad (46)$$

where $\lambda$ is a real-valued positive constant, $f(y)$ and $g(y)$ denote two real-valued functions that are assumed to be infinitely differentiable, and the quantity $y_0$ stands for the value of $y$ for which $df(y)/dy = 0$. Also in (46), $\ddot{f}(y_0)$ represents the second derivative of the function $f(y)$ with respect to the variable $y$ evaluated at $y_0$. It is important to note that the LCR $N_R(r)$ in (24) fulfills all conditions of the Laplace theorem. Therefore, a comparison of (24) and (46) yields

$$\begin{cases} \lambda = 1 \\ f(y) = \frac{\sqrt{A_{q_1}}}{2q_1\Omega_1}\left(\frac{r}{y}\right)^2 G(\theta_1) + \frac{\sqrt{A_{q_2}}}{2q_2\Omega_2}y^2 G(\theta_2) \\ g(y) = \frac{1}{y}\sqrt{\left(\frac{r}{y}\right)^2 F(\theta_2) + y^2 F(\theta_1)}. \end{cases} \quad (47)$$

After some algebraic manipulations, we can present the quantities $y_0, f(y_0)$, $g(y_0)$, and $\ddot{f}(y_0)$ in the following form

$$\begin{cases} y_0 = \left(\frac{A_{q_1}}{A_{q_2}}\right)^{\frac{1}{8}}\left(\frac{q_2 G(\theta_1)}{q_1 G(\theta_2)}\right)^{\frac{1}{4}}\sqrt{\sqrt{\frac{\Omega_2}{\Omega_1}}r} \\ f(y_0) = \frac{(A_{q_1}A_{q_2})^{\frac{1}{4}}}{\sqrt{\Omega_1\Omega_2}}\sqrt{\frac{G(\theta_1)G(\theta_2)}{q_1 q_2}}\,r \\ g(y_0) = \sqrt{\left(\frac{A_{q_2}}{A_{q_1}}\right)^{\frac{1}{2}}\frac{q_1\Omega_1 G(\theta_2)}{q_2\Omega_2 G(\theta_1)}F(\theta_2) + F(\theta_1)} \\ \ddot{f}(y_0) = \frac{4\sqrt{A_{q_2}}}{q_2\Omega_2}G(\theta_2). \end{cases} \quad (48)$$

After substituting (48) in (46), we obtain the approximate closed-form solution in (25) for the LCR $N_R(r)$ of double Hoyt fading processes $R(t)$.

## APPENDIX B

In this Appendix, we present the derivation of the SEP $\bar{P}_s$ of square M-QAM modulation schemes over double Hoyt fading channels. By substituting (29) and (36) in (28), $\bar{P}_s$ can be written as

$$\begin{aligned} \bar{P}_s = {} & 4\left(1-\frac{1}{\sqrt{M}}\right)\frac{\sqrt{A_{q_1}A_{q_2}}}{2\pi^2\bar{\gamma}}\int_0^\pi d\theta_1\int_0^\pi d\theta_2\int_0^\infty d\gamma \\ & Q\left(\sqrt{2g_{QAM}\gamma}\right) \\ & \times K_0\left(\frac{1}{2}\sqrt{\frac{\gamma}{\bar{\gamma}}}\sqrt{\left(A_{q_1}-B_{q_1}\cos(\theta_1)\right)\left(A_{q_2}-B_{q_2}\cos(\theta_2)\right)}\right) \\ & -4\left(1-\frac{1}{\sqrt{M}}\right)^2\frac{\sqrt{A_{q_1}A_{q_2}}}{2\pi^2\bar{\gamma}}\int_0^\pi d\theta_1\int_0^\pi d\theta_2\int_0^\infty d\gamma \\ & Q^2\left(\sqrt{2g_{QAM}\gamma}\right) \\ & \times K_0\left(\frac{1}{2}\sqrt{\frac{\gamma}{\bar{\gamma}}}\sqrt{\left(A_{q_1}-B_{q_1}\cos(\theta_1)\right)\left(A_{q_2}-B_{q_2}\cos(\theta_2)\right)}\right). \end{aligned} \quad (49)$$

Using the alternate definite integral form of the Gaussian $Q$-function given by [30, eq. (4.2)]

$$Q(x) = \frac{1}{\pi}\int_0^{\pi/2} \exp\left(-\frac{x^2}{2\sin^2(\theta)}\right) d\theta, \quad x \geq 0 \qquad (50)$$

and its corresponding square described by [30, eq. (4.9)]

$$Q^2(x) = \frac{1}{\pi}\int_0^{\pi/4} \exp\left(-\frac{x^2}{2\sin^2(\theta)}\right) d\theta, \quad x \geq 0 \qquad (51)$$

the expression (49) becomes

$$\begin{aligned}\bar{P}_s = {} & 4\left(1-\frac{1}{\sqrt{M}}\right)\frac{\sqrt{A_{q_1}A_{q_2}}}{2\pi^2\bar{\gamma}} \\ & \left(\int_0^{\pi} d\theta_1 \int_0^{\pi} h\left(\theta_1,\theta_2,g_{QAM},\bar{\gamma},\frac{\pi}{2}\right) d\theta_2\right. \\ & \left. -\left(1-\frac{1}{\sqrt{M}}\right)\int_0^{\pi} d\theta_1 \int_0^{\pi} h\left(\theta_1,\theta_2,g_{QAM},\bar{\gamma},\frac{\pi}{4}\right) d\theta_2\right)\end{aligned} \qquad (52)$$

where the function $h\left(\theta_1,\theta_2,g_{QAM},\bar{\gamma},\alpha\right)$ is given by

$$\begin{aligned}& h\left(\theta_1,\theta_2,g_{QAM},\bar{\gamma},\alpha\right) \\ & = \frac{1}{\pi}\int_0^{\alpha} d\theta_3 \int_0^{\infty} \exp\left(-\frac{g_{QAM}\gamma}{\sin^2(\theta_3)}\right) \\ & \times K_0\left(\frac{1}{2}\sqrt{\frac{\gamma}{\bar{\gamma}}}\sqrt{\left(A_{q_1}-B_{q_1}\cos(\theta_1)\right)\left(A_{q_2}-B_{q_2}\cos(\theta_2)\right)}\right) d\gamma.\end{aligned} \qquad (53)$$

Using [38, eqs. (6.614.4) and (8.338.1)] and [39, eq. (13.18.5)], the semi-infinite range integral in (53) can be solved and $h\left(\theta_1,\theta_2,g_{QAM},\bar{\gamma},\alpha\right)$ can be written as

$$\begin{aligned}& h(\theta_1,\theta_1,g_{QAM},\bar{\gamma},\alpha) \\ & = \frac{1}{2\pi g_{QAM}}\int_0^{\alpha} \sin^2(\theta_3) d\theta_3 \\ & \times\Gamma\left(0,\frac{\sin^2(\theta_3)}{16 g_{psk}\bar{\gamma}}(A_{q_1}-B_{q_1}\cos(\theta_1))(A_{q_2}-B_{q_2}\cos(\theta_2))\right) \\ & \times\exp\left(\frac{\sin^2(\theta_3)}{16 g_{psk}\bar{\gamma}}(A_{q_1}-B_{q_1}\cos(\theta_1))(A_{q_2}-B_{q_2}\cos(\theta_2))\right).\end{aligned} \qquad (54)$$

Finally, substituting (54) in (52) yields the SEP $\bar{P}_s$ in (37).

## ACKNOWLEDGMENT

This paper was presented at the 6th IEEE International Symposium on Wireless Communication Systems, Siena, Italy, September 2009 [1, pp. 201–205].

## REFERENCES

[1] N. Hajri, N. Youssef, and M. Pätzold, "A study on the statistical properties of double Hoyt fading channels," in *Proc. 6th IEEE Int. Symp. Wireless Commun. Syst.*, Siena, Italy, Sep. 2009, pp. 201–205.
[2] P. Almers, F. Tufvesson, and A. F. Molisch, "Keyhole effect in MIMO wireless channels: Measurements and theory," *IEEE Trans. Wireless. Commun.*, vol. 5, no. 12, pp. 3596–3604, Dec. 2006.
[3] D. Chizhik, G. J. Foschini, M. J. Gans, and R. A. Valenzuela, "Keyholes, correlations, and capacities of multielement transmit and receive antennas," *IEEE Trans. Wireless Commun.*, vol. 1, no. 2, pp. 361–368, Apr. 2002.
[4] J. Salo, H. M. El-Sallabi, and P. Vainikainen, "Statistical analysis of the multiple scattering radio channel," *IEEE Trans. Antennas Propag.*, vol. 54, no. 11, pp. 3114–3124, Nov. 2006.
[5] W. Honcharenko, H. L. Bertoni, and J. L. Dailing, "Bilateral averaging over receiving and transmitting areas for accurate measurements of sector average signal strength inside buildingS," *IEEE Trans. Antennas. Propag.*, vol. 43, no. 5, pp. 508–512, May 1995.
[6] V. Erceg, S. J. Fortune, J. Ling, A. J. Rustako, and R. A. Valenzuela, "Comparisons of a computer-based propagation prediction tool with experimental data collected in urban microcellular environments," *IEEE J. Sel. Areas Commun.*, vol. 15, no. 4, pp. 677–684, May 1997.
[7] I. Z. Kovacs, "Radio channel characterization for private mobile radio systems," Ph.D. dissertation, Dept. Commun. Theory, Aalborg Univ., Aalborg, Denmark, 2002.
[8] J. Maurer, T. Fügen, and W. Wiesbeck, "Narrow-band measurement and analysis of the inter-vehicle transmission channel at 5.2 GHz," in *Proc. 55th IEEE Veh. Technol. Conf. (VTC-Spring)*, vol. 3. Birmingham, AL, USA, May 2002, pp. 1274–1278.
[9] D. W. Matolak and J. Frolik, "Worse-than-Rayleigh fading: Experimental results and theoretical models," *IEEE Commun. Mag.*, vol. 49, no. 4, pp. 140–146, Apr. 2011.
[10] Y. Alghorani, G. Kaddoum, S. Muhaidat, and S. Pierre, "On the approximate analysis of energy detection over $n*$ Rayleigh fading channels through cooperative spectrum sensing," *IEEE Wireless Commun. Lett.*, vol. 4, no. 4, pp. 413–416, Aug. 2015.
[11] A. Sendonaris, E. Erkip, and B. Aazhang, "User cooperation diversity. Part I. System description," *IEEE Trans. Commun.*, vol. 51, no. 11, pp. 1927–1938, Nov. 2003.
[12] J. N. Laneman, D. N. C. Tse, and G. W. Wornell, "Cooperative diversity in wireless networks: Efficient protocols and outage behavior," *IEEE Trans. Inf. Theory*, vol. 50, no. 12, pp. 3062–3080, Dec. 2004.
[13] C. S. Patel, G. L. Stüber, and T. G. Pratt, "Statistical properties of amplify and forward relay fading channels," *IEEE Trans. Veh. Technol.*, vol. 55, no. 1, pp. 1–9, Jan. 2006.
[14] B. Talha and M. Pätzold, "Channel models for mobile-to-mobile cooperative communication systems: A state of the art review," *IEEE Veh. Technol. Mag.*, vol. 6, no. 2, pp. 33–34, Jun. 2011.
[15] D. Kim, M. A. Ingram, and W. W. Smith, "Measurements of small-scale fading and path loss for long range RF tags," *IEEE Trans. Antennas Propag.*, vol. 51, no. 8, pp. 1740–1749, Aug. 2003.
[16] A. Bekkali, S. Zou, A. Kadri, M. Crisp, and R. V. Penty, "Performance analysis of passive UHF RFID systems under cascaded fading channels and interference effects," *IEEE Trans. Wireless Commun.*, vol. 14, no. 3, pp. 1421–1433, Mar. 2015.
[17] N. C. Sagias and G. S. Tombras, "On the cascaded Weibull fading channel model," *J. Franklin Inst.*, vol. 344, pp. 1–11, Jan. 2007.
[18] B. Talha and M. Pätzold, "Statistical modeling and analysis of mobile-to-mobile fading channels in cooperative networks under line-of-sight conditions," *Wireless Pers. Commun.*, vol. 54, no. 1, pp. 3–19, 2010.
[19] Z. Hadzi-Velkov, N. Zlatanov, and G. K. Karagiannidis, "On the second order statistics of the multihop Rayleigh fading channel," *IEEE Trans. Commun.*, vol. 57, no. 6, pp. 1815–1823, Jun. 2009.
[20] G. K. Karagiannidis, N. C. Sagias, and P. T. Mathiopoulos, "$N*$Nakagami: A novel stochastic model for cascaded fading channels," *IEEE Trans. Commun.*, vol. 55, no. 8, pp. 1453–1458, Aug. 2007.
[21] N. Zlatanov, Z. Hadzi-Velkov, and G. K. Karagiannidis, "Level crossing rate and average fade duration of the double Nakagami-$m$ random process and application in MIMO keyhole fading channels," *IEEE Commun. Lett.*, vol. 12, no. 11, pp. 822–824, Nov. 2008.
[22] K. Peppas, F. Lazarakis, A. Alexandridis, and K. Dangakis, "Cascaded generalised-K fading channel," *IET Commun.*, vol. 4, no. 1, pp. 116–124, 2010.

[23] Y. A. Chau and K. Y.-T. Huang, "On the second-order statistics of correlated cascaded Rayleigh fading channels," *Int. J. Antennas Propag.*, vol. 2012, Jun. 2012, Art. no. 108534.
[24] F. J. Lopez-Martinez, E. Kurniawan, R. Islam, and A. Goldsmith, "Average fade duration for amplify-and-forward relay networks in fading channels," *IEEE Trans. Wireless Commun.*, vol. 14, no. 10, pp. 5454–5467, Oct. 2015.
[25] R. S. Hoyt, "Probability functions for the modulus and angle of the normal complex variate," *Bell Syst. Tech. J.*, vol. 26, no. 2, pp. 318–359, Apr. 1947.
[26] B. Chytil, "The distribution of amplitude scintillation and the conversion of scintillation indices," *J. Atmos. Terrestrial Phys.*, vol. 29, no. 9, pp. 1117–1175, Sep. 1967.
[27] N. Youssef, C.-X. Wang, and M. Pätzold, "A study on the second order statistics of Nakagami-Hoyt mobile fading channels," *IEEE Trans. Veh. Technol.*, vol. 54, no. 4, pp. 1259–1265, Jul. 2005.
[28] M. Nakagami, "The *m*-distribution—A general formula of intensity distribution of rapid fading," in *Statistical Methods in Radio Wave Propagation*. New York, NY, USA: Pergamon, 1960, pp. 3–36.
[29] J. F. Paris, "Nakagami-*q* (Hoyt) distribution function with applications," *Electron. Lett.*, vol. 45, no. 4, pp. 210–211, Feb. 2009.
[30] M. K. Simon and M.-S. Alouini, *Digital Communication Over Fading Channels*, 2nd ed. Hoboken, NJ, USA: Wiley, 2004.
[31] K. T. Hemachandra and N. C. Beaulieu, "Simple expressions for the SER of dual MRC in correlated Nakagami-*q* (Hoyt) fading," *IEEE Commun. Lett.*, vol. 14, no. 8, pp. 743–745, Aug. 2010.
[32] R. Subadar and P. R. Sahu, "Performance analysis of dual MRC receiver in correlated Hoyt fading channels," *IEEE Commun. Lett.*, vol. 13, no. 6, pp. 405–407, Jun. 2009.
[33] J. M. Romero-Jerez and F. J. Lopez-Martinez, "A new framework for the performance analysis of wireless communications under Hoyt (Nakagami-*q*) fading," *IEEE Trans. Inf. Theory*, vol. 63, no. 3, pp. 1693–1702, Mar. 2017.
[34] R. A. A. de Souza, M. D. Yacoub, and G. S. Rabelo, "Bivariate Hoyt (Nakagami-*q*) distribution," *IEEE Trans. Commun.*, vol. 60, no. 3, pp. 714–722, Mar. 2012.
[35] R. Wong, *Asymptotic Approximations of Integrals*. Philadelphia, PA, USA: SIAM, 2001.
[36] M. K. Simon, *Probability Distributions Involving Gaussian Random Variables: A Handbook for Engineers and Scientists*. Dordrecht, The Netherlands: Kluwer, 2002.
[37] A. Papoulis and S. U. Pillai, *Probability, Random Variables and Stochastic Processes*, 4th ed. New York, NY, USA: McGraw-Hill, 2002.
[38] I. S. Gradshteyn and I. M. Ryzhik, *Tables of Integrals, Series and Products*, 5th ed. New York, NY, USA: Academic, 1994.
[39] F. W. J. Olver, D. W. Lozier, R. F. Boisvert, and C. W. Clark, *NIST Handbook of Mathematical Functions*, 1st ed. New York, NY, USA: Cambridge Univ. Press, 2010.
[40] S. O. Rice, "Mathematical analysis of random noise," *Bell Syst. Tech. J.*, vol. 23, no. 3, pp. 282–332, 1944.
[41] S. O. Rice, "Mathematical analysis of random noise," *Bell Syst. Tech. J.*, vol. 24, no. 1, pp. 46–156, 1945.
[42] M. Pätzold, *Mobile Radio Channels*, 2nd ed. Chichester, U.K.: Wiley, 2011.
[43] W. C. Jakes, *Microwave Mobile Communications*, 2nd ed. Piscataway, NJ, USA: IEEE Press, 1993.
[44] N. Hajri, N. Youssef, F. Choubani, and T. Kawabata, "BEP performance of M2M communications over frequency flat double Hoyt fading channels," in *Proc. 21st Annu. IEEE Int. Symp. Pers., Indoor Mobile Radio Commun. (PIMRC)*, Istanbul, Turkey, Sep. 2010, pp. 1962–1966.

**NAZIH HAJRI** received the Dipl.-Ing., M.E., and Ph.D. degrees from the Ecole Supérieure des Communications de Tunis, Tunisia, in 2004, 2005, and 2011, respectively, all in telecommunications. In 2009, he joined the Higher Institute of Computer Science and Mathematics, Monastir, Tunisia, where he is currently an Assistant Professor. He is also a member of the Innovation of Communicant and Cooperative Mobiles Laboratory, Ecole Supérieure des Communications de Tunis. His research interests include wireless channel modeling and simulation, performance analysis of wireless communications, mobile-to-mobile communications, and noise theory.

**NEJI YOUSSEF** received the B.E. degree in telecommunications from the Ecole des Postes et des Télécommunications de Tunis, Tunisia, in 1983, the D.E.A. degree in electrical engineering from the Ecole Nationale d'Ingénieurs de Tunis, in 1986, and the M.E. and Ph.D. degrees in communication engineering from the University of Electro-Communications, Tokyo, Japan, in 1991 and 1994, respectively. From 1994 to 1996, he was a Research Associate with the University of Electro-Communications. In 1997, he joined the Ecole Supérieure des Communications de Tunis, where he is currently a Professor. His research interests include noise theory, modeling of multipath fading channels, and the performance analysis of wireless communications.

**TSUTOMU KAWABATA** (M'93) was born in Toyama, Japan, in 1955. He received the B.E., M.E., and D.E. degrees in mathematical engineering from The University of Tokyo, in 1978, 1980, and 1993, respectively. He joined the University of Electro-Communications in 1982, where he is currently a Professor with the Department of Communication Engineering and Informatics. He was a Visitor at Stanford University from 1987 to 1989 and from 1996 to 1997, at the Eindhoven University of Technology in 1995, and at INRIA in 1996. His research interests lie in information and communication theory and include quantizations, rate-distortions, lossless data compressions, and bio-informatics.

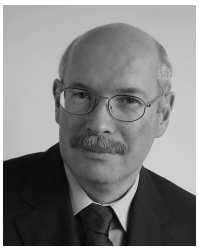

**MATTHIAS PÄTZOLD** (M'94–SM'98) received the Dipl.-Ing. and Dr.-Ing. degrees in electrical engineering from Ruhr-University Bochum, Bochum, Germany, in 1985 and 1989, respectively, and the Habilitation degree in communications engineering from the Technical University of Hamburg-Harburg, Germany, in 1998. From 1990 to 1992, he was with ANT Nachrichtentechnik GmbH, Backnang, Germany, where he was involved in digital satellite communications. From 1992 to 2001, he was with the Department of Digital Networks, Technical University of Hamburg-Harburg. Since 2001, he has been a Full Professor of mobile communications with the University of Agder, Norway. He has authored several books and numerous technical papers. His publications received 13 best paper awards. He has been actively participating in numerous conferences, serving as a member and as a chair of technical program committees.

**WIEM DAHECH** received the B.E. degree in computer networks and telecommunications from the Institut National des Sciences Appliquées et de la Techologie, Tunisia, in 2011, and the M.S. degree in electronic systems and communication networks from the Ecole Polytechnique de Tunisie, in 2012. She is currently pursuing the Ph.D. degree with the Ecole Supérieure des Communications de Tunis, Tunisia.